Supporting Information:

Through Space Charge-Transfer Emission in Lambda (Λ)-Shaped Triarylboranes and the Use in Fluorescent Sensing for Fluoride and Cyanide ions

He Xi,[a,b] Yang Liu,[b] Chun-Xue Yuan,[c] Ye-Xin Li,[d] Lei Wang,[b] Xu-Tang Tao,*[b] Xiao-Hua Ma,*[a] Chun-Fu Zhang*[e] and Yue Hao*[a, e]

[a] School of Advanced Materials and Nanotechnology, Xidian University, 2 South Taibai Road, Xi'an 710071, P. R. China, Email: xhma@xidian.edu.cn

[b] State Key Laboratory of Crystal Materials, Shandong University, Jinan 250100, P. R. China, Email: txt@sdu.edu.cn

[c] College of Materials Science and Engineering, Tongji University, Caoan Road 4800, Shanghai, 201804, P. R. China.

[d] School of Chemistry and Chemical Engineering, Jinan University, Jinan 250022, P. R. China

[e] Key Lab of Wide Band-Gap Semiconductor Materials and Devices, Xidian University, 2 South Taibai Road, Xi'an 710071, P. R. China, Email: cfzhang@xidian.edu.cn, yhao@xidian.edu.cn

Table of Contents

Photophysical properties

Solvent dependent absorption and PL spectra of TBBN, TBBN2, TBB and TBNN.

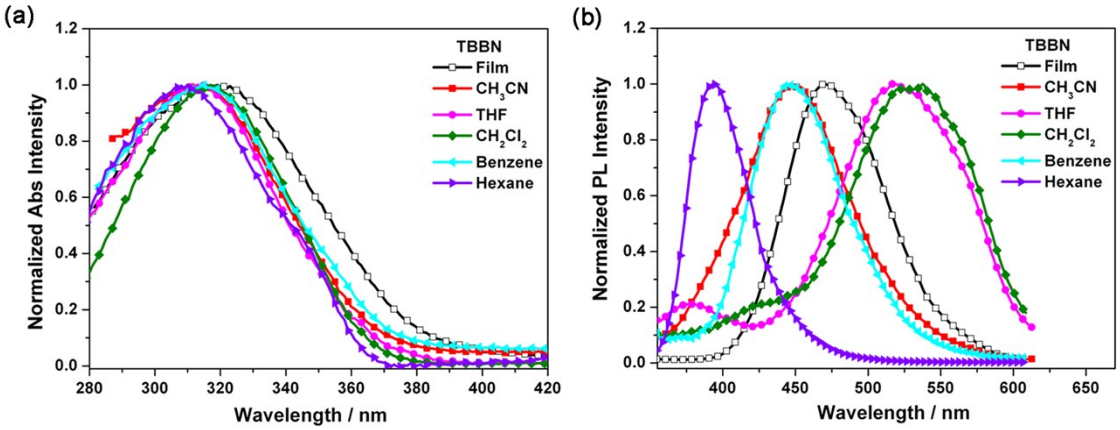

Fig. S1. Absorption (a) and PL spectra (b) of **TBBN** in various solvents and thin film.

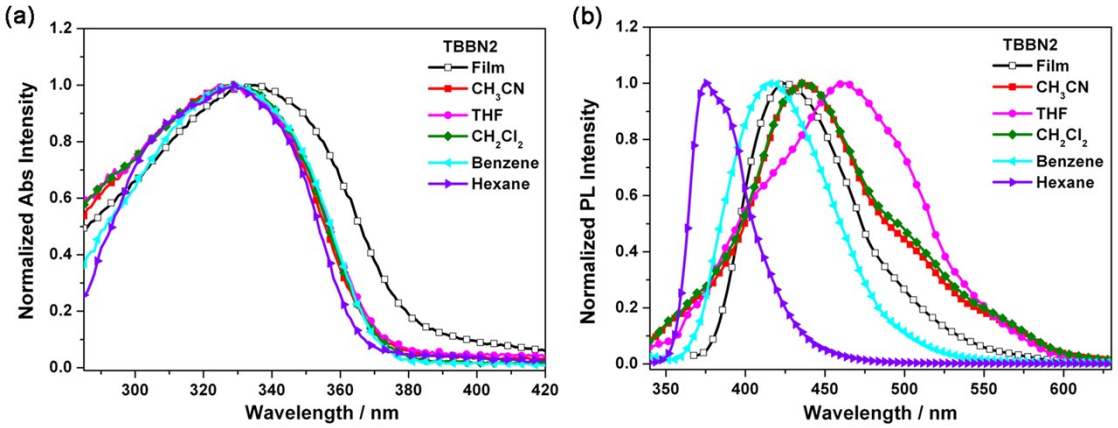

Fig. S2. Absorption (a) and PL spectra (b) of **TBBN2** in various solvents and thin film.

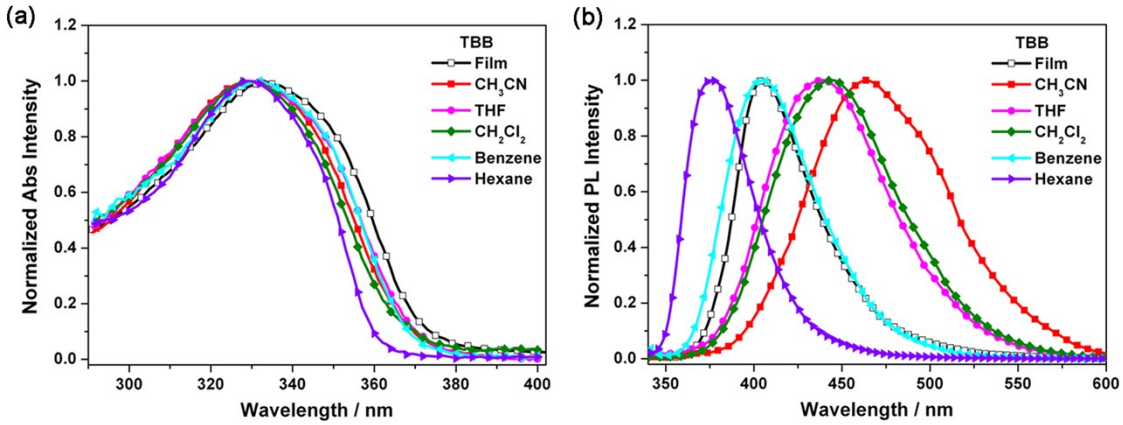

Fig. S3. Absorption (a) and PL spectra (b) of **TBB** in various solvents and thin film.

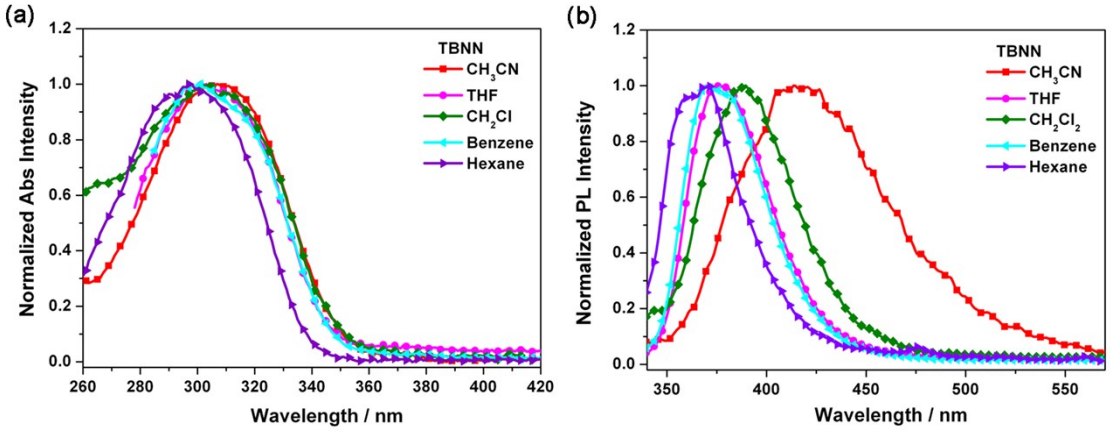

Fig. S4. Absorption (a) and PL spectra (b) of **TBNN** in various solvents.

Table S1. Absorption and PL Data o**f TBBN, TBBN2, TBB and TBNN.**

Compound	Solvent	λ_{abs} (nm)	λ_{em} (nm)	$\triangle\nu$ (cm^{-1}) [c]	Φ_F [d]
TBBN	Hexane	310	394[a]	6877	0.17
	Benzene	315	445 [a]	9274	0.14
	CH_2Cl_2	317	538 [a]	12958	0.11
	THF	313	518 [a]	12607	0.09
	MeCN	314	447 [a]	9476	0.10
	Film	319	470	10071	0.07
TBBN2	Hexane	329	375 [b]	3728	0.26
	Benzene	328	418 [b]	6564	0.21
	CH_2Cl_2	330	437 [b]	7420	0.14
	THF	327	460 [b]	8983	0.11
	MeCN	328	436 [b]	7552	0.07
	Film	335	424	6266	0.05
TBB	Hexane	329	375	3728	0.70
	Benzene	332	405	5368	0.88
	CH_2Cl_2	329	444	7873	0.78
	THF	330	438	7472	0.80
	MeCN	331	463	8613	0.56
	Film	333	405	5339	0.04
TBNN	Hexane	297	371	6716	0.51
	Benzene	301	370	6196	0.65
	CH_2Cl_2	304	389	7188	0.60
	THF	303	376	6408	0.58
	MeCN	307	414	8419	0.42

[a]Excited at 313 nm. [b] Excited at 328 nm. [c] Stokes shift. [d] Absolute quantum yields which were determined by a calibrated integrating sphere system.

Theoretical Calculations

The TD-DFT calculations on **TBB**, **TBBN** and **TBBN2** were performed using the Gaussian 09 program at the B3LYP/6-31G(d) level of theory using the optimized structure geometry. The time-dependent density functional theory (TD-DFT) calculations were conducted at the B3LYP/6-31G(d) level of theory to understand their intramolecular CT transitions.

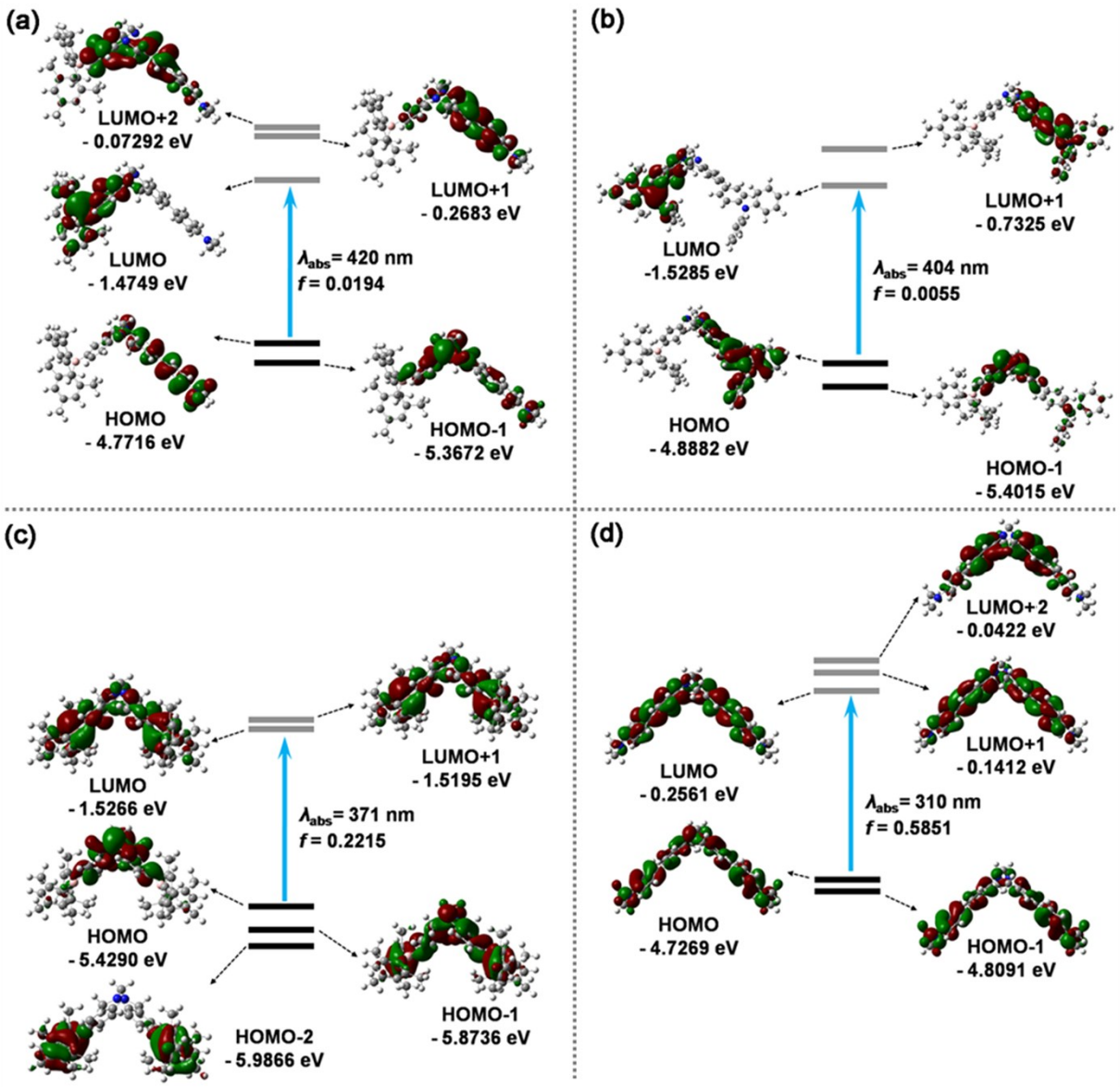

Fig. S5. Calculated molecular orbitals of (a) **TBBN**, (b) **TBBN2**, (c) **TBB** and (d) **TBNN**. The transition energies and oscillator strengths (*f*) were calculated at the B3LYP/6-31G(d) level of theory.

Table S2. Calculated transition energies, absorption wavelengths, oscillator strength and assignments for compounds **TBBN**, **TBBN2**, **TBB** and **TBNN** calculated at the B3LYP/6-31G level of thoery.

Compound	Excited state	Transition energies (eV)	Absorption(nm) (oscillator strengths)	Assignments (%)
TBBN	1	**2.95**	**420 (0.0194)**	**HOMO→LUMO (69)**
				HOMO-1→LUMO (12)
	2	3.42	362 (0.161)	HOMO-1→LUMO (68)
				HOMO→LUMO (12)
	3	3.64	362 (0.161)	HOMO-3→LUMO (61)
				HOMO-2→LUMO (32)
	4	3.76	330 (0.1242)	HOMO-2→LUMO (48)
				HOMO-4→LUMO (38)
				HOMO-3→LUMO (30)
	5	3.88	320 (0.0774)	HOMO-4→LUMO (51)
				HOMO-5→LUMO (40)
				HOMO-2→LUMO (24)
	6	3.97	312 (0.0088)	HOMO-6→LUMO (70)
	7	4.04	330 (0.1026)	HOMO-5→LUMO (54)
				HOMO-2→LUMO (27)
				HOMO-4→LUMO (26)
	8	**4.09**	**303 (0.2269)**	**HOMO→LUMO+1 (52)**
				HOMO→LUMO+2 (34)
	9	**4.20**	**295 (0.4618)**	**HOMO→LUMO+2 (53)**
				HOMO→LUMO+1 (38)
TBBN2	1	**3.07**	**404 (0.0055)**	**HOMO→LUMO (68)**
				HOMO-1→LUMO (17)
	2	3.37	368 (0.1674)	HOMO-1→LUMO (67)
				HOMO→LUMO (68)
	3	**3.62**	**342 (0.3408)**	**HOMO-3→LUMO (55)**
				HOMO-2→LUMO (32)
				HOMO→LUMO+1 (28)
	4	**3.66**	**338 (0.5517)**	**HOMO→LUMO+1 (61)**
				HOMO-3→LUMO (33)
TBB	1	**3.34**	**370 (0.2215)**	**HOMO→LUMO (70)**
	2	3.39	366 (0.0472)	HOMO→LUMO+1 (70)
	3	**3.67**	**337 (0.2693)**	**HOMO-2→LUMO (47)**
				HOMO-3→LUMO+1 (37)
				HOMO-1→LUMO+1 (37)
TBNN	1	**3.99**	**311 (0.5851)**	**HOMO→LUMO (66)**
				HOMO→LUMO+1 (15)
	2	4.16	298 (0.0002)	HOMO-1→LUMO (51)
				HOMO→LUMO+1 (42)
	3	4.22	294 (0.2593)	HOMO→LUMO+2 (63)

X-ray Crystallography

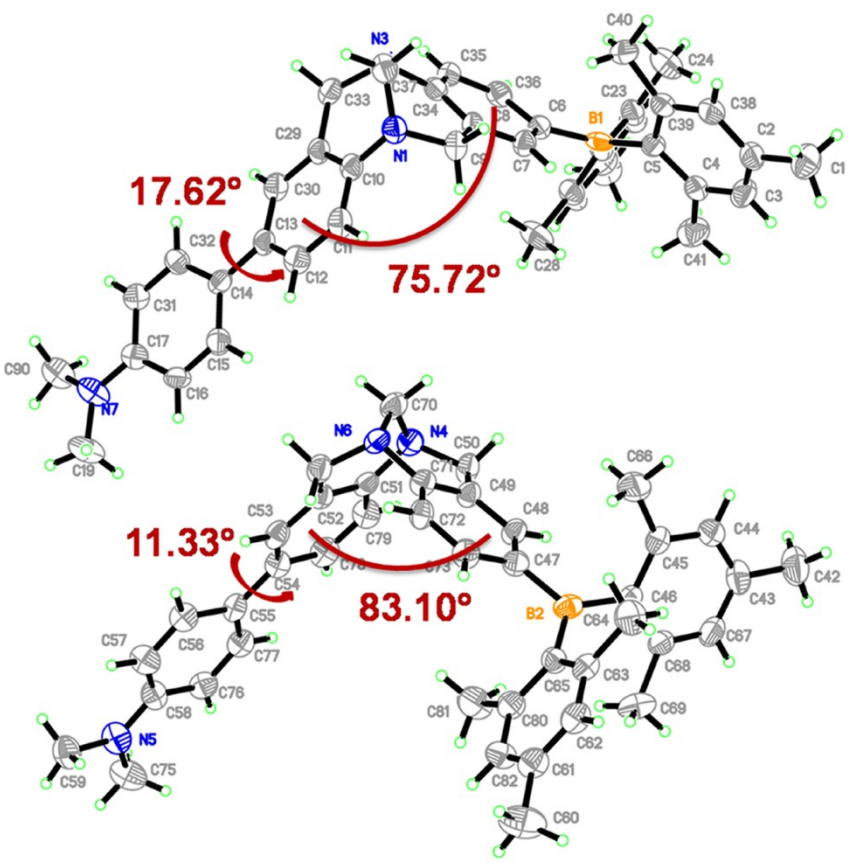

Fig. S6. ORTEP drawing of **TBBN** showing the 30% probability ellipsoids and labeling schemes.

Table S3. Crystal data, diffraction data, and refinement data of **TBBN**.

Compound	TBBN
Chemical formula	$C_{41}H_{44}BN_3$
Formula weight	589.60
Crystal system	Triclinic
Space group	$P\bar{1}$
a/Å	8.660(12)
b/Å	15.52(2)
c/Å	25.74(4)
α(°)	100.726(19)
β(°)	96.95(2)
γ(°)	93.252(19)
Unit cell volume/ Å^3	3363(8)
T/K	296(2)
Z	4
D_{calcd}/Mg m^{-3}	1.165
Radiation type	Mo Kα (λ = 0.71073Å)
Absorption coefficient, μ/mm^{-1}	0.067
F(000)	1264
θ range for data collection(°)	1.34 to 27.79
Limiting indices	$-11 \le h \le 11$ $-20 \le k \le 20$ $-33 \le l \le 33$
Reflections collected/unique	40641/15634 [R(int) = 0.2267]
Final R indices (I >2σ(I))	R_1 = 0.0693, wR_2 = 0.1102
Final R indices (all data)	R_1 = 0.3894, wR_2 = 0.1964
Max. and min. transmission	0.9983 and 0.9879
Data/restraints/parameters	15634 / 0 / 827
Goodness of fit on F^2	0.832
Largest diff. peak and hole/e Å^3	0.187 and -0.219
CCDC number	905360

Table S4. Prominent weak intermolecular forces for packing structure of **TBBN**.

Number	Weak intermolecular interactions	Distance/Å		Shift distance[c] /Å	Angle[d] (°)	Type
1	π···π(C55～C77)	3.900(7)[a]	3.762(2)[b]	1.025	15.24	A*-A*
2	π···π(C14～C32)	3.727(7)[a]	3.692(2)[b]	0.505	7.78	A-A

[a] the distance between the centroids of the two π rings; [b] the vertical distance between the two π rings; [c] the slippage distance between ring (I) and perpendicular project of ring (J) on ring (I); [d] the sliding angle of the two π rings.

Titration Measurement

Titration of TBBN with TBAF

The titration experiments were carried out in a THF solution of **TBBN** (4.722 μM, 2 mL in a quartz cuvette). Then the solution was titrated with incremental amounts of fluoride ion by addition of a concentrated TBAF solution in THF (4.16×10^{-4} M), in which **TBBN** was also included at its initial concentration to avoid the dilution effects. The fluorescence band at 518 nm and 378 nm were monitored (λ_{ex}= 313 nm).

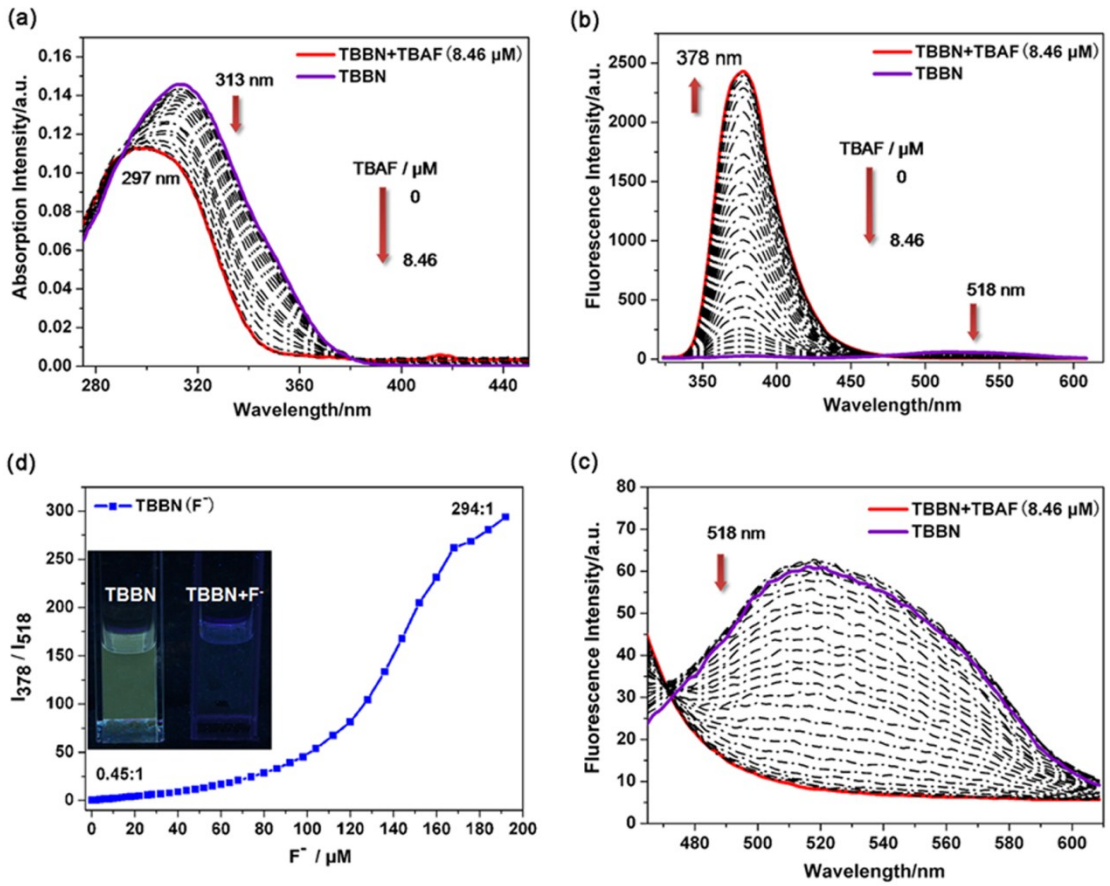

Fig. S7. The absorption (a) and PL (b) spectral changes of **TBBN** (4.722 μM in THF, λ_{ex}=313nm) upon addition of TBAF solution (4.16×10^{-4} M). (c) The enlarged view of the PL spectrum change at 518 nm (d) Plot of fluorescence intensity ratio (I_{378}/I_{518}) versus concentration of F^-. Inset in (d): Photograph of THF solution of **TBBN** before and after addition of F^- with 365 nm irradiation.

Determination of Binding Constants

To determine the binding constants, the equations described by Connors[1] were used. Based on this, a plot of $(1-I/I_o)/[F]$ vs I/I_o was made. The intensity of the native fluorescence peak in THF at 518 nm was used as the initial intensity (I_0), and the intensity of the new fluorescence band at 378 nm as the final intensity (I).

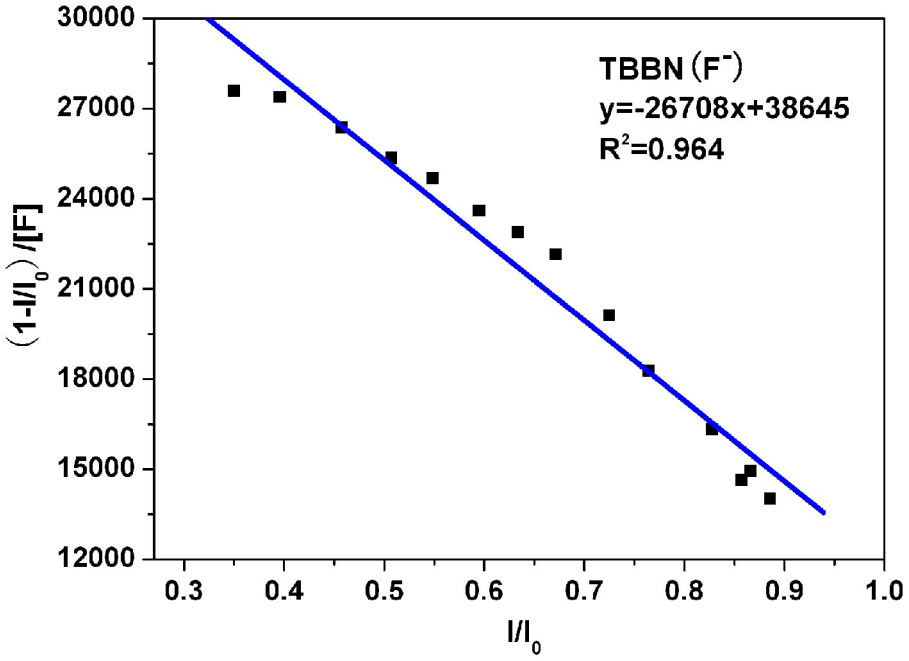

Fig. S8. Plot of $(1-I/I_o)/[F]$ vs I/I_o of **TBBN** upon addition of TBAF. From the slope of $(1-I/I_o)/[F]$ vs I/I_o, a binding constant **$K= 2.67\times10^4\ M^{-1}$** was obtained.

Titration of TBBN with TBACN

The titration experiments on **TBBN** upon addition of TBACN were the same as on TBAF. A THF solution of **TBBN** (4.661 μM, 2 mL) was placed in a quartz cuvette and titrated with incremental amounts of cyanide ion by the addition of a concentrated TBACN solution in THF (4.531×10^{-4} M), in which **TBBN** was also included at its initial concentration to avoid dilution effects. The fluorescence band at 518 nm and 378 nm were monitored (λ_{ex}= 313 nm).

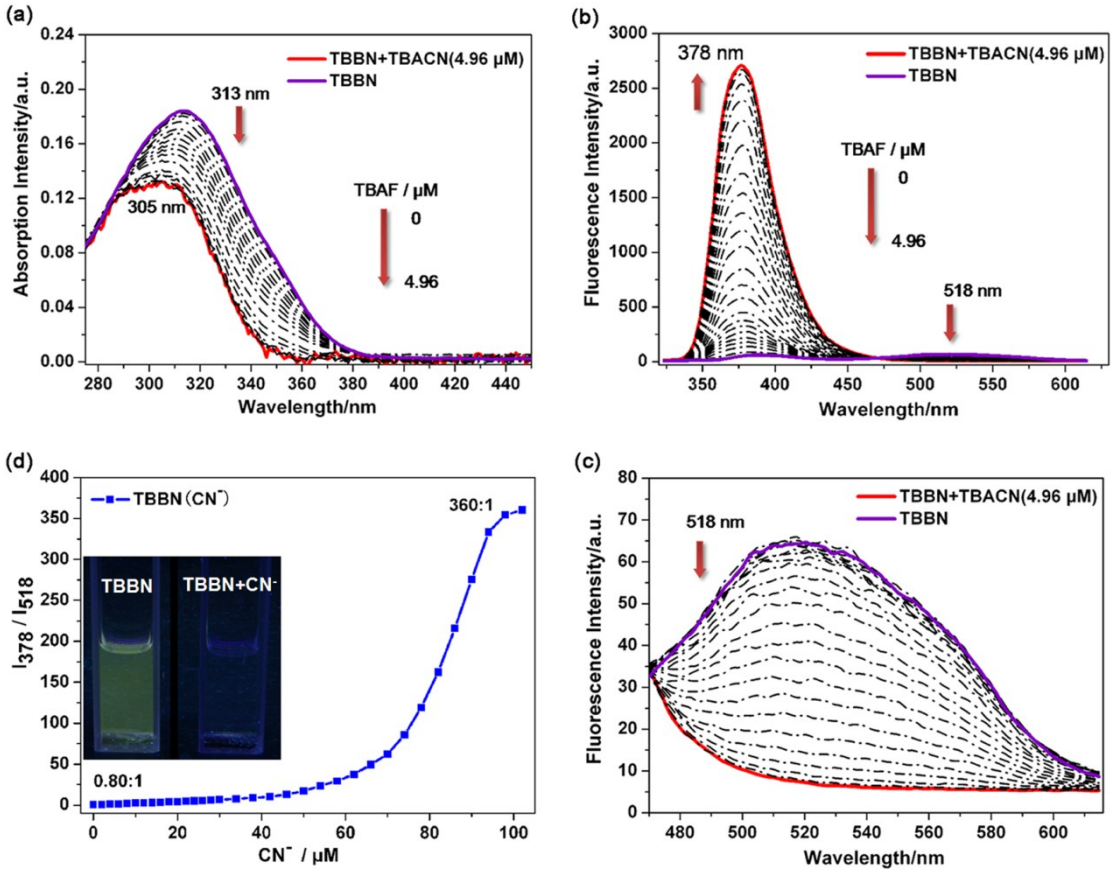

Fig. S9. The absorption (a) and PL (b) spectral changes of **TBBN** (4.661 μM in THF, λ_{ex}=313nm) upon addition of TBACN solution (4.531×10^{-4} M). (c) The enlarged view of the PL spectrum change at 518 nm (d) Fluorescence intensity ratio (I_{378}/I_{518}) versus concentration of CN^-. Inset in (d): Photographs of THF solution of **TBBN** before and after addition of CN^- with 365 nm irradiation.

Determination of Binding Constants

Based on the equations described by Connors[1], a plot of $(1-I/I_o)/[CN]$ vs I/I_o was made. The intensity of the native fluorescence peak in THF at 518 nm was used as the initial intensity (I_0), and the intensity of the new fluorescence band at 378 nm as the final intensity (I).

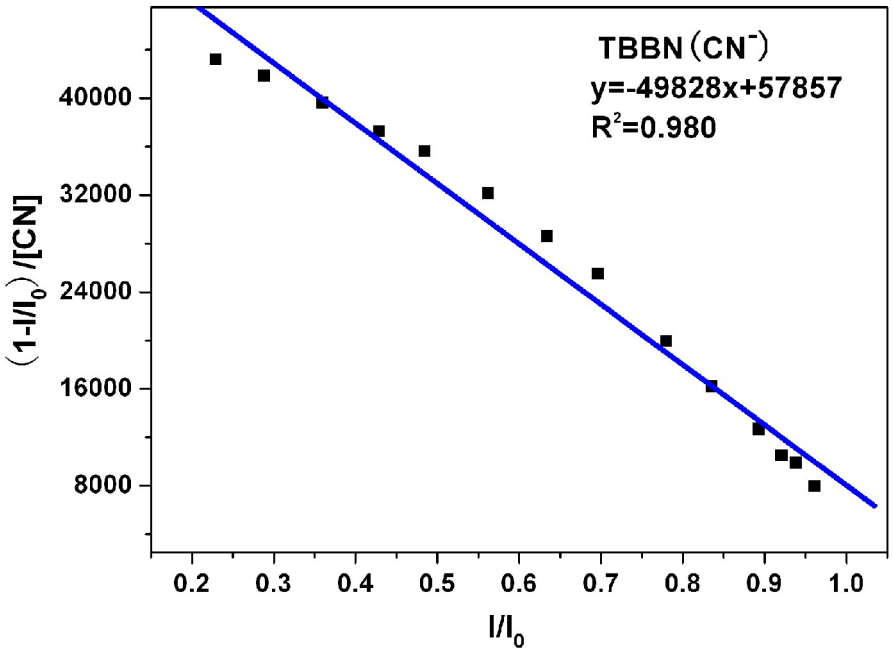

Fig. S10. Plot of $(1-I/I_o)/[CN]$ vs I/I_o of **TBBN** upon addition of TBACN. From the slope of $(1-I/I_o)/[CN]$ vs I/I_o, a binding constant **K= 5.0×10^4 M^{-1}** was obtained.

Titration of TBBN2 with TBAF

The titration experiments were carried out in a THF solution of **TBBN2** (2.099 μM, 2 mL in a quartz cuvette). Then the solution was titrated with incremental amounts of fluoride ion by addition of a concentrated TBAF solution in THF (4.22×10^{-4} M), in which **TBBN2** was also included at its initial concentration to avoid dilution effects. The fluorescence band at 460 nm and 388 nm were monitored (λ_{ex}= 328 nm).

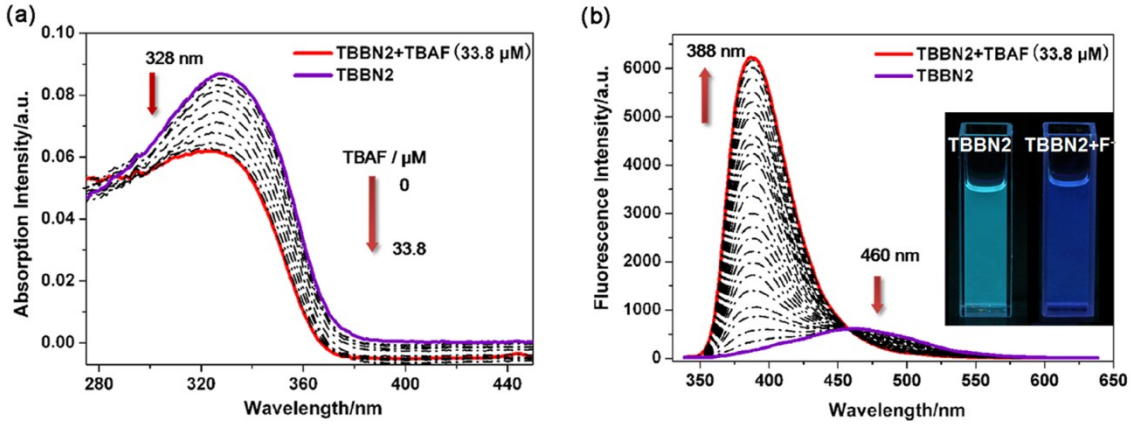

Fig. S11. The absorption (a) and PL (b) spectral changes of **TBBN2** (2.099μM in THF, λ_{ex}=328nm) upon addition of TBAF solution (4.22×10^{-4} M). Inset in (b): Photographs of THF solution of **TBBN2** before and after addition of F^- with 365 nm irradiation.

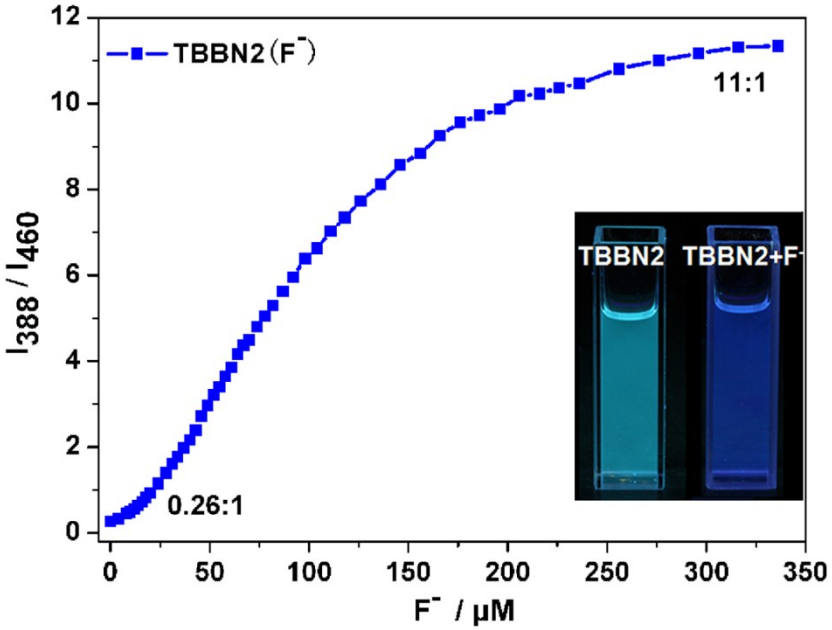

Fig. S12. Plot of fluorescence intensity ratio (I_{388}/I_{460}) of **TBBN2** versus concentration of F^-.

Determination of Binding Constants

To determine the binding constants, the equations described by Connors[1] were used. Based on this, a plot of $(1-I/I_o)/[F]$ vs I/I_o was made. The intensity of the native fluorescence peak in THF at 460 nm was used as the initial intensity (I_0), and the intensity of the new fluorescence band at 388 nm as the final intensity (I).

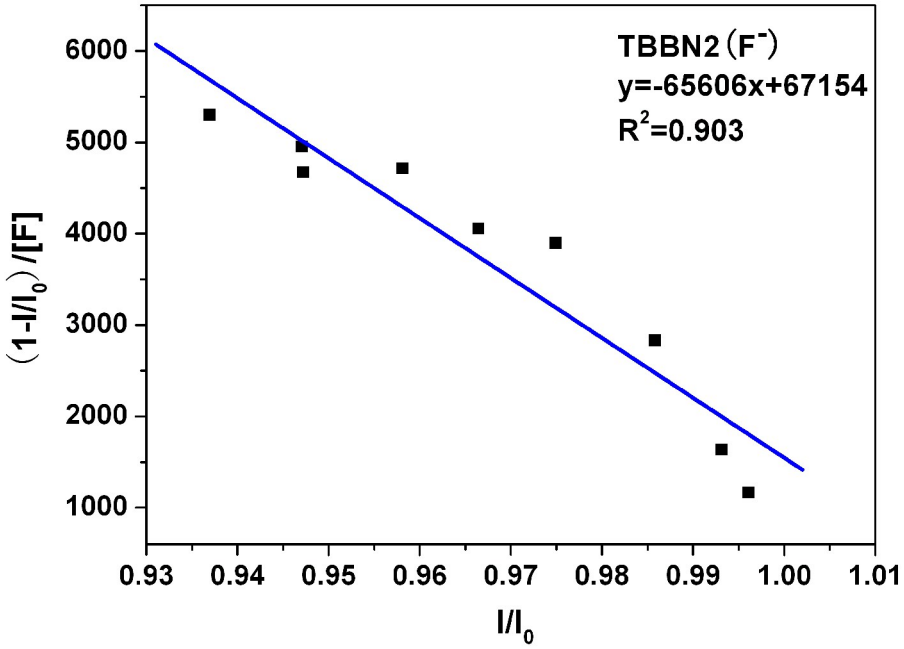

Fig. S13. Plot of $(1-I/I_o)/[F]$ vs I/I_o of **TBBN2** upon addition of TBAF. From the slope of $(1-I/I_o)/[F]$ vs I/I_o, a binding constant **K= 6.56×10^4 M^{-1}** was obtained.

Titration of TBBN2 with TBACN

The titration experiments on **TBBN2** upon addition of TBACN were the same as on TBAF. A THF solution of **TBBN2** (2.099 μM, 2 mL) was placed in a quartz cuvette and titrated with incremental amounts of cyanide ions by the addition of a concentrated TBACN solution in THF (6.64×10^{-4} M), in which **TBBN2** was also included at its initial concentration to avoid dilution effects. The fluorescence band at 460 nm and 388 nm were monitored (λ_{ex}= 328 nm).

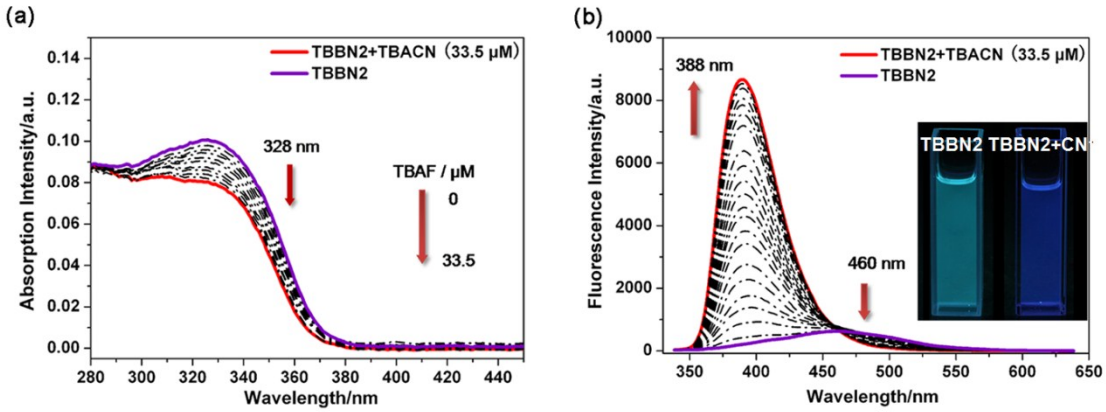

Fig. S14. The absorption (a) and PL (b) spectral changes of **TBBN2** (2.099 μM in THF, λ_{ex}=328nm) upon addition of TBACN solution (6.64×10^{-4} M). Inset in (b): Photographs of THF solution of **TBBN2** before and after addition of CN^- with 365 nm irradiation.

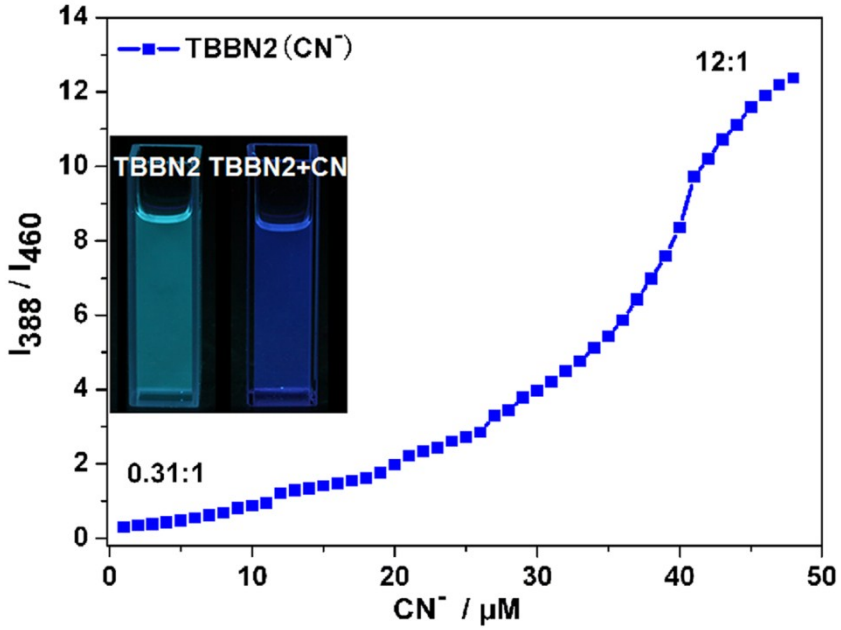

Fig. S15. Plot of fluorescence intensity ratio (I_{388}/I_{460}) of **TBBN2** versus concentration of CN^-.

Determination of Binding Constants

Based on the equations described by Connors[1], a plot of $(1-I/I_o)/[CN]$ vs I/I_o was made. The intensity of the native fluorescence peak in THF at 460 nm was used as the initial intensity (I_0), and the intensity of the new fluorescence band at 388 nm as the final intensity (I).

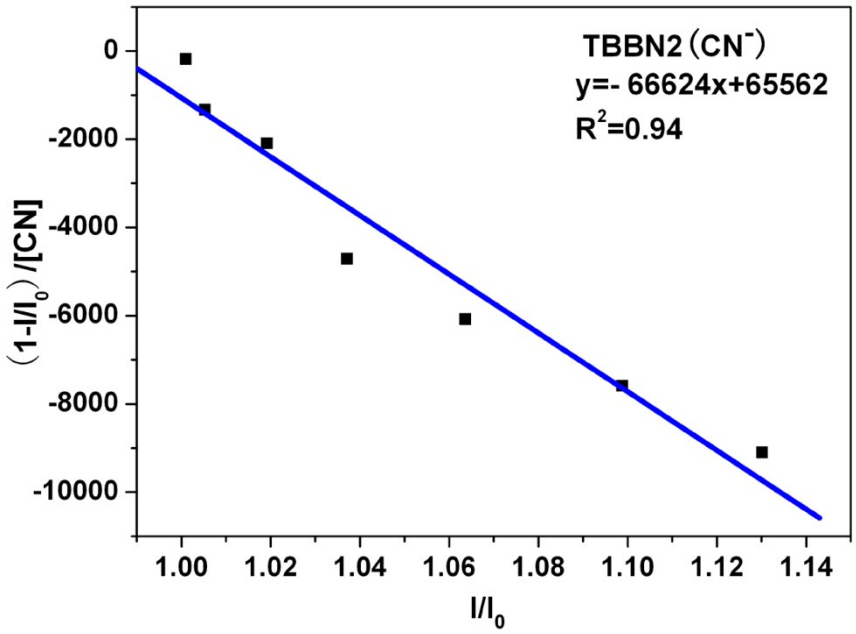

Fig. S16. Plot of $(1-I/I_o)/[CN]$ vs I/I_o of **TBBN2** upon addition of TBACN. From the slope of $(1-I/I_o)/[CN]$ vs I/I_o, a binding constant **$K= 6.66\times10^4\ M^{-1}$** was obtained.

Titration of TBB with TBAF

The titration experiments were carried out in a THF solution of **TBB** (4.372 μM, 2 mL in a quartz cuvette). Then the solution was titrated with incremental amounts of fluoride ion by the addition of a concentrated TBAF solution in THF (4.24×10^{-4} M), in which **TBB** was also included at its initial concentration to avoid dilution effects. The fluorescence band at 388 nm was monitored (λ_{ex}= 330 nm).

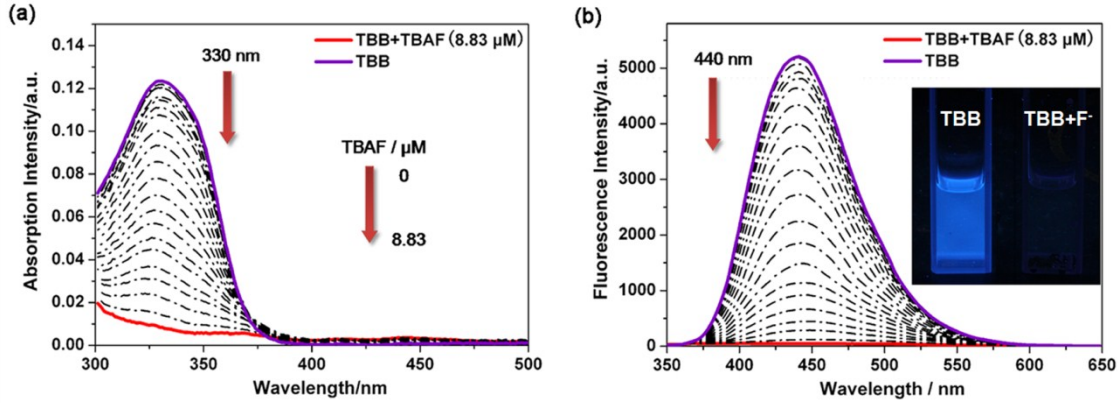

Fig. S17. The absorption (a) and PL (b) spectral changes of **TBB** (4.372 μM in THF, λ_{ex}= 330nm) upon addition of TBAF solution (4.24×10^{-4} M). The inset in (b) shows the photographs of THF solution of **TBB** before and after addition of F^- with 365 nm irradiation.

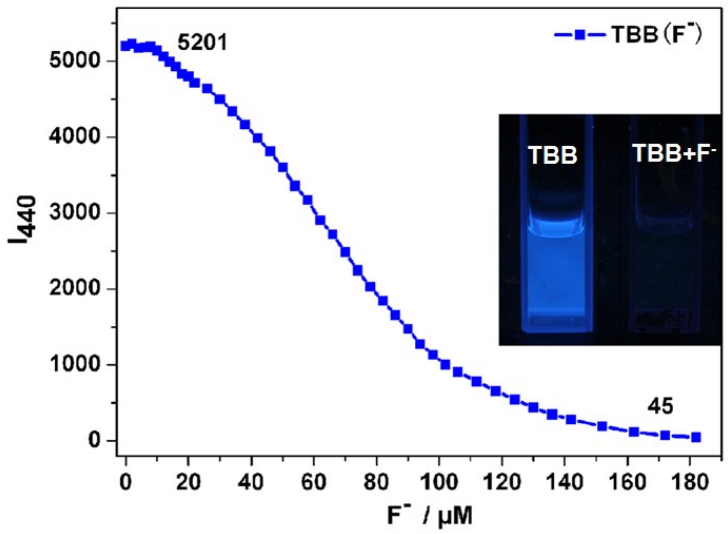

Fig. S18. Plot of fluorescence intensity change of **TBB** at 440 nm (I_{440}) versus concentration of F^-.

Determination of Binding Constants

To determine the binding constants, the equations described by Connors[1] were used. Based on this, a plot of $(1-I/I_o)/[F]^2$ vs I/I_o was made. The fluorescence intensity at 440 nm was used as the initial intensity (I_0), and the intensity change at 440 nm upon addition of TBAF as the final intensity (I).

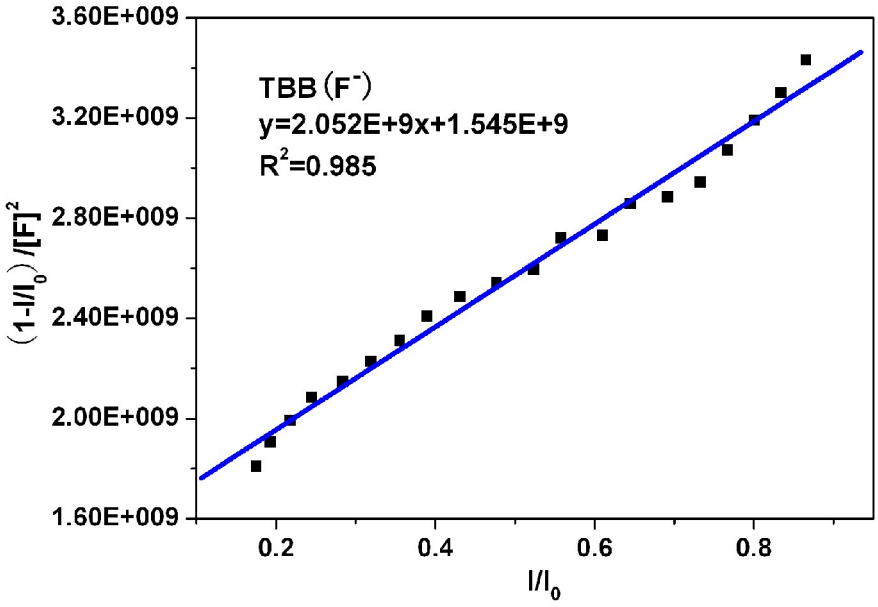

Fig. S19. Plot of $(1-I/I_o)/[F]^2$ vs I/I_o of **TBB** upon addition of TBAF. From the slope of $(1-I/I_o)/[F]^2$ vs I/I_o, a binding constant **K= 2.05×10^9 M^{-2}** was obtained.

Titration of TBB with TBACN

The titration experiments on **TBB** upon addition of TBACN were the same as on TBAF. A THF solution of **TBB** (4.698 μM, 2 mL) was placed in a quartz cuvette and titrated with incremental amounts of cyanide ion by addition of a concentrated TBACN solution in THF (4.45×10^{-4} M), in which **TBB** was also included at its initial concentration to avoid dilution effects. The fluorescence band at 388 nm was monitored (λ_{ex}= 330 nm).

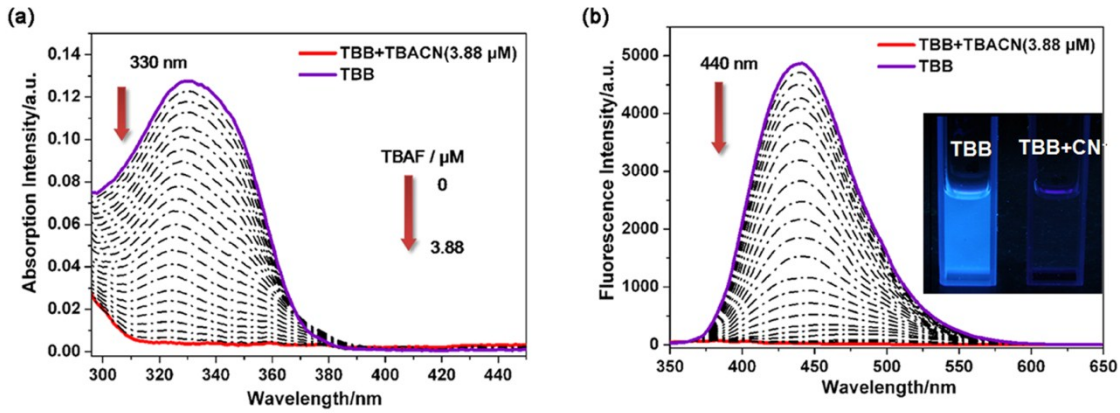

Fig. S20. The absorption (a) and PL (b) spectral changes of **TBB** (4.698 μM in THF, λ_{ex}= 330nm) upon addition of TBACN solution(4.45×10^{-4} M). The inset in (b) shows the photographs of THF solution of **TBB** before and after addition of CN^- with 365 nm irradiation.

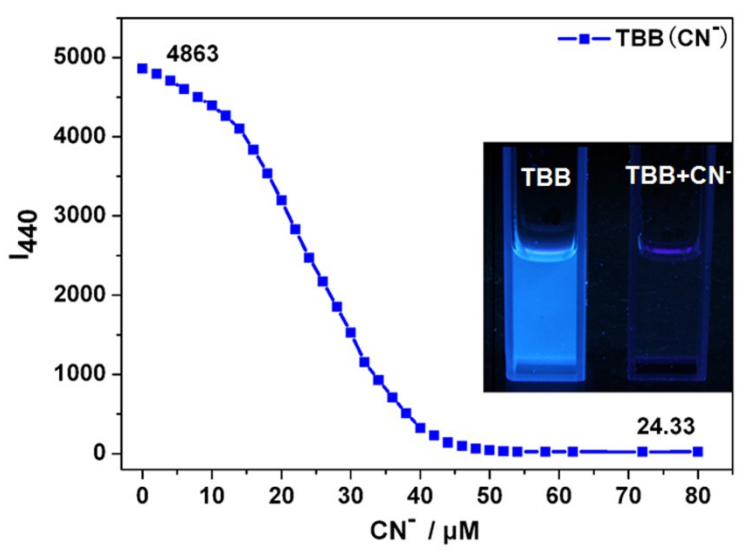

Fig. S21. Plot of fluorescence intensity change of **TBB** at 440 nm (I_{440}) versus concentration of CN^-.

Determination of Binding Constants

Based on the equations described by Connors[1], a plot of $(1-I/I_o)/[CN]^2$ vs I/I_o was made. The fluorescence intensity at 440 nm was used as the initial intensity (I_0), and the intensity change at 440 nm upon addition of TBACN as the final intensity (I).

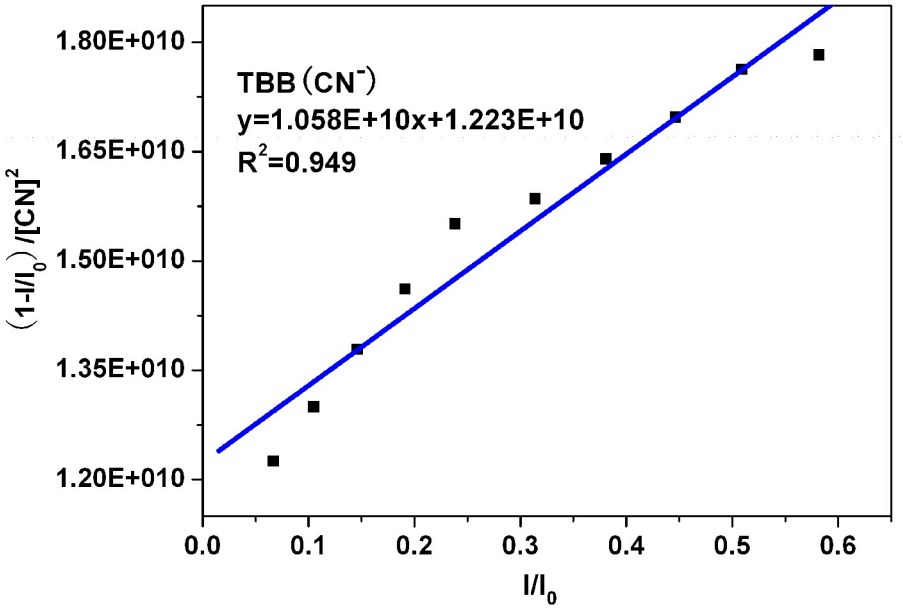

Fig. S22. Plot of $(1-I/I_o)/[CN]^2$ vs I/I_o of **TBB** upon addition of TBACN. From the slope of $(1-I/I_o)/[CN]^2$ vs I/I_o, a binding constant **K= 1.06×10^{10} M^{-2}** was obtained.

NMR Titrations of TBBN, TBBN2 and TBB with fluoride

^{19}F NMR Titration of TBBN with fluoride ion in CD_2Cl_2

All the ^{19}F NMR titration experiments were recorded with a Bruker 300 spectrometer in CD_2Cl_2. To a CD_2Cl_2 solution of TBAF (0.013 M, 1 mL) in the NMR tube, incremental amounts of **TBBN** powder were added to produce **TBBN** solutions with concentrations of 0.0020 M, 0.0042 M, 0.0067 M, 0.0092 M, 0.012 M and 0.016 M. When there was no ^{19}F NMR spectral change observed in the process, excess TBACl was added ([TBACl]/[TBAF]=2.64) to investigate the selectivity of **TBBN** for fluoride. The ^{19}F NMR spectral change was monitored during the whole experiment, and the signals for free F^- and bound F^- were recorded. It was noted that about 1 equivalent of **TBBN** was needed to consume all of the starting fluoride ion, indicating the formation of a 1:1 complex.

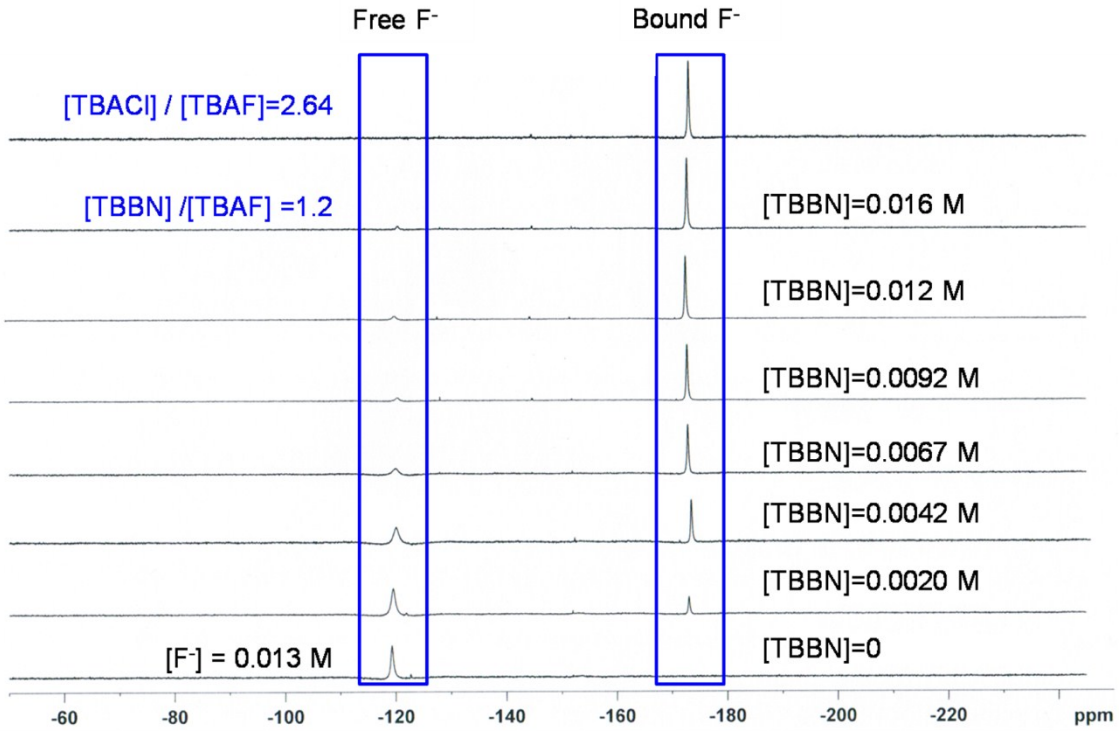

Fig. S23. ^{19}F NMR spectra of **TBBN** before and after the addition of TBAF in CD_2Cl_2. The top is the ^{19}F NMR spectrum of **TBBN** after the addition of TBACl ([TBACl]/[TBAF]=2.64).

^{19}F NMR Titration of TBBN2 with fluoride ion in CD_2Cl_2

To a CD_2Cl_2 solution of TBAF (0.013 M, 1 mL) in the NMR tube, incremental amounts of **TBBN2** powder were added to produce **TBBN2** solutions with concentrations of 0.0020 M, 0.0042 M, 0.0065 M, 0.0086 M, 0.011 M and 0.013 M. When there was no ^{19}F NMR spectral change observed in the process, excess TBACl was added ([TBACl]/[TBAF]=2) to investigate the selectivety of **TBBN2** for fluoride. The ^{19}F NMR spectral change was monitored during the whole experiment, and the signals for free F^- and bound F^- were recorded. It was noted that about 1 equivalent of **TBBN2** was needed to consume all of the starting fluoride ion, indicating the formation of a 1:1 complex.

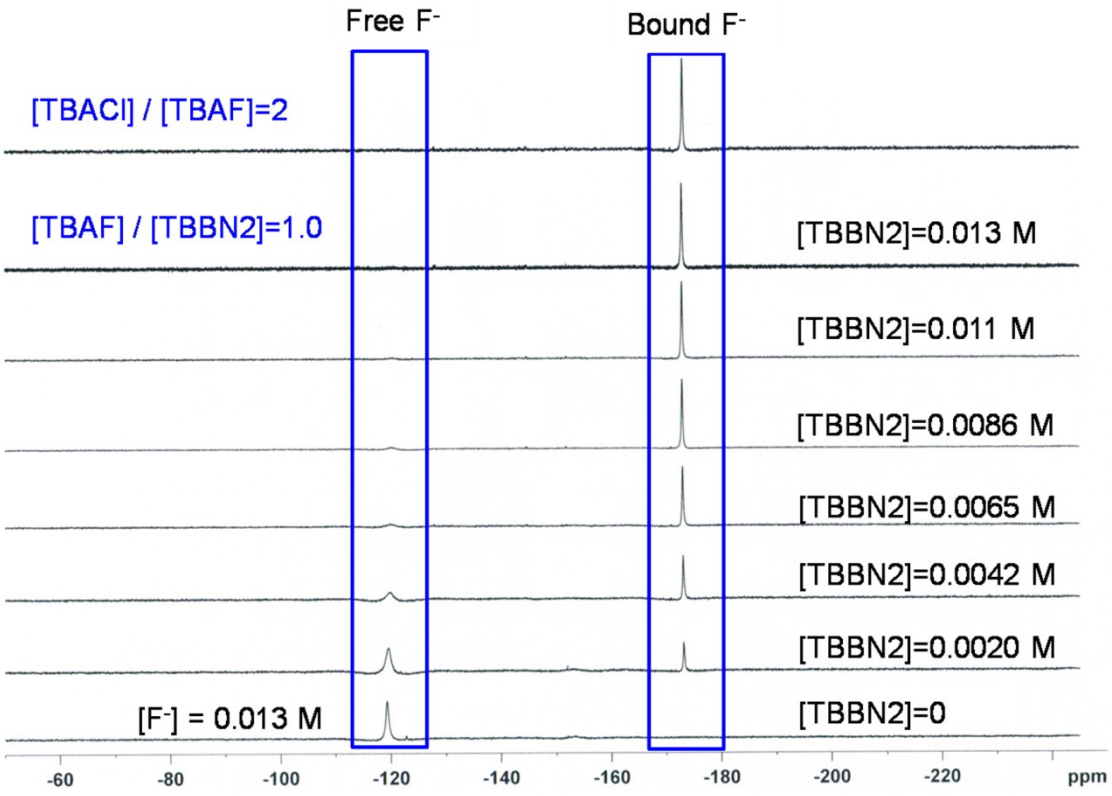

Fig. S24. ^{19}F NMR spectra of **TBBN2** before and after the addition of TBAF in CD_2Cl_2. The top is the ^{19}F NMR spectrum of **TBBN2** after the addition of TBACl ([TBACl]/[TBAF]=2).

^{19}F NMR Titration of TBB with fluoride ion in CD_2Cl_2

To a CD_2Cl_2 solution of TBAF (0.025 M, 1 mL) in the NMR tube, incremental amounts of **TBB** powder were added to produce the **TBB** solutions with concentrations of 0.0020 M, 0.0041 M, 0.0064 M, 0.0089 M, and 0.011 M. When there was no ^{19}F NMR spectral change observed in the process, excess TBACl was added ([TBACl]/[TBAF]=1.98) to investigate the selectivety of **TBB** for fluoride. The ^{19}F NMR spectral change was monitored during the whole experiment, and the signals for free F^- and bound F^- were recorded. It was noted that about 0.5 equivalent of **TBB** was needed to consume all of the starting fluoride ion, indicating the formation of a 2:1 complex.

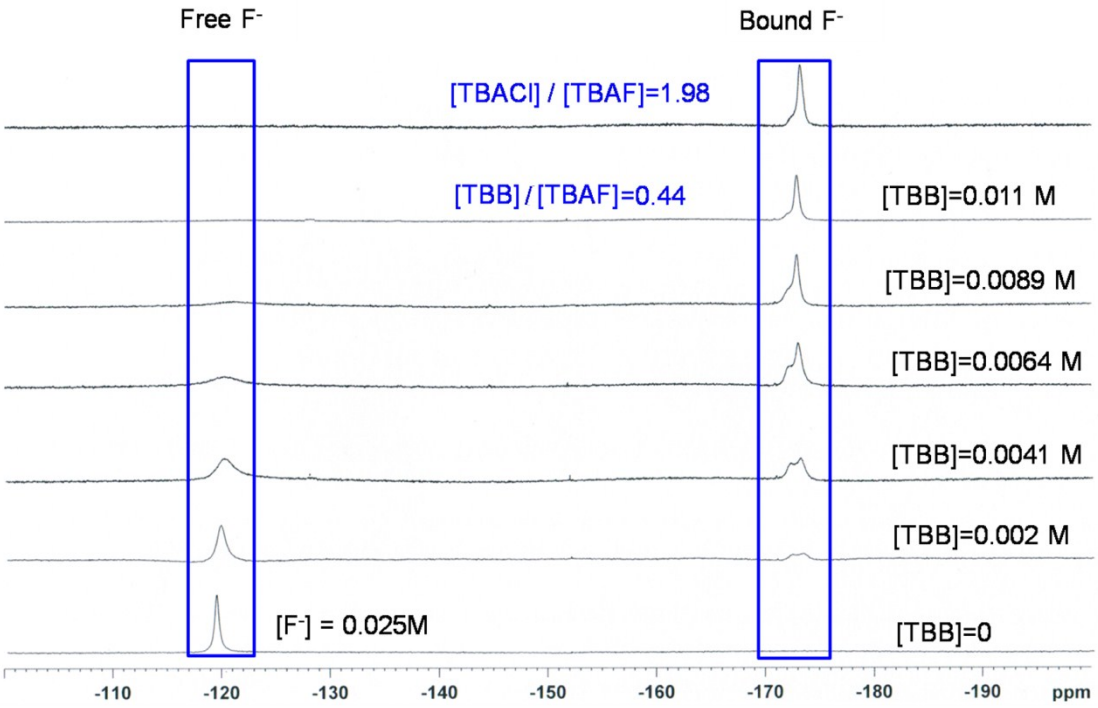

Fig. S25. ^{19}F NMR spectra of **TBB** before and after the addition of TBAF in CD_2Cl_2. The top is the ^{19}F NMR spectrum of **TBB** after the addition of TBACl ([TBACl]/[TBAF]=1.98).

Titration of TBBN with various anions.

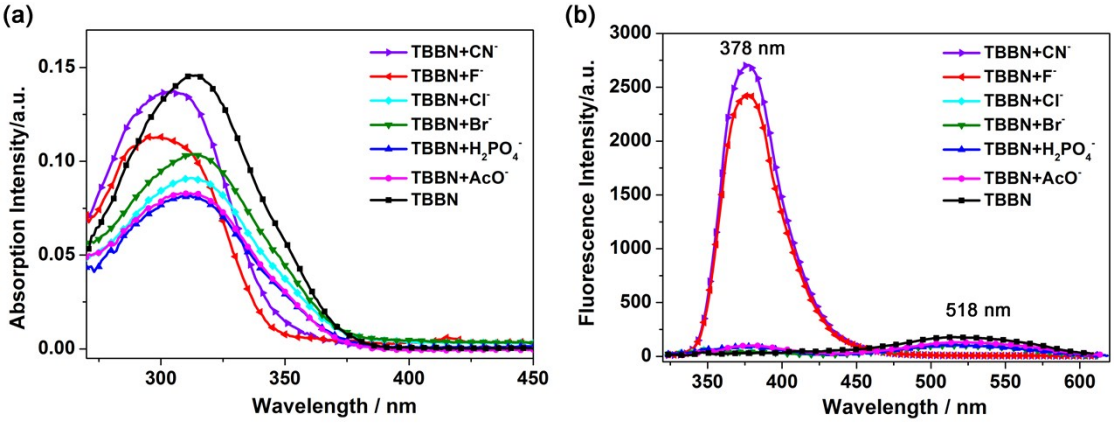

Fig. S26. Absorption (a) and PL (b) spectral changes of **TBBN** (2.09 μM in THF, λ_{ex}=313nm) upon addition of an excess of acetate, phosphate, bromide, chloride, fluoride and cyanide ions in THF solutions (193 μM). All the anions were used as tetrabutylammonium salts.

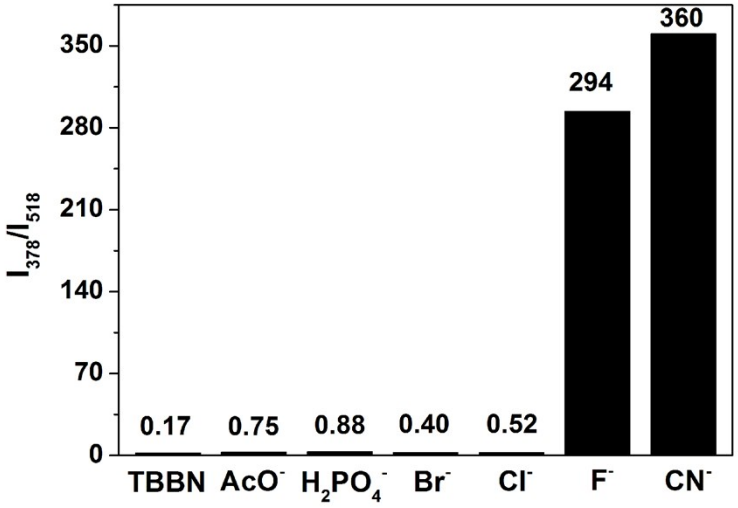

Fig. S27. A comparison of fluorescence intensity ratio (I_{378}/I_{518}) of **TBBN** in THF solution (2.09 μM) upon addition of an excess of various anions (193 μM). Plot clearly indicates that **TBBN** shows higher selectivity for F^- and CN^- over Cl^-, Br^-, AcO^- and $H_2PO_4^-$.

Titration of TBBN2 with various anions.

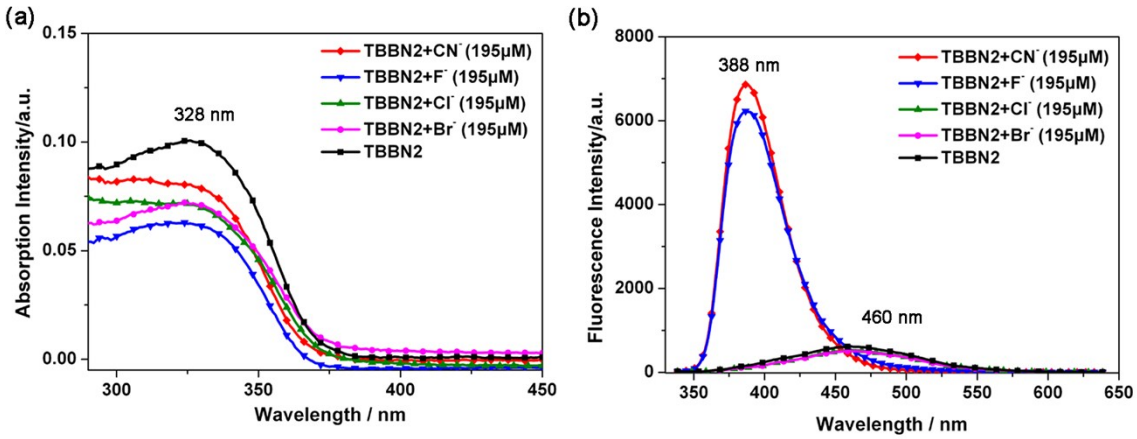

Fig. S28. Absorption (a) and PL (b) spectral changes of **TBBN2** (2.15 μM in THF, λ_{ex}=328nm) upon addition of an excess of bromide, chloride, fluoride and cyanide ions in THF solutions (195 μM).

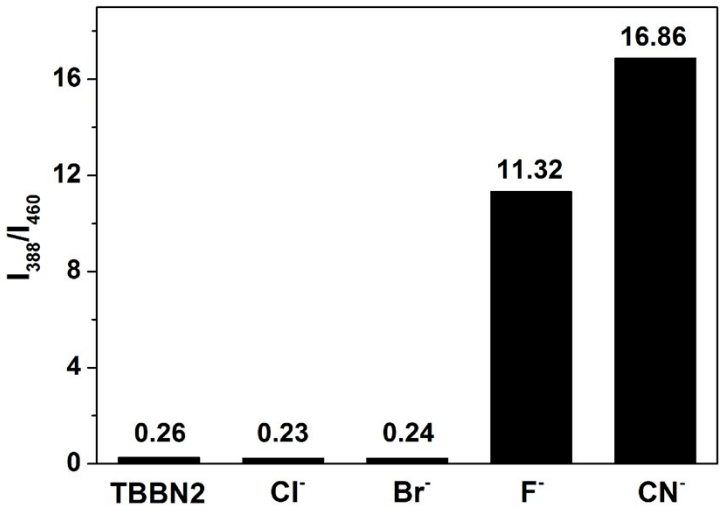

Fig. S29. A comparison of fluorescence intensity ratio (I_{388}/I_{460}) of **TBBN2** in THF solution (2.15 μM) after addition of an excess of various anions (195 μM).

Titration of TBB with various anions.

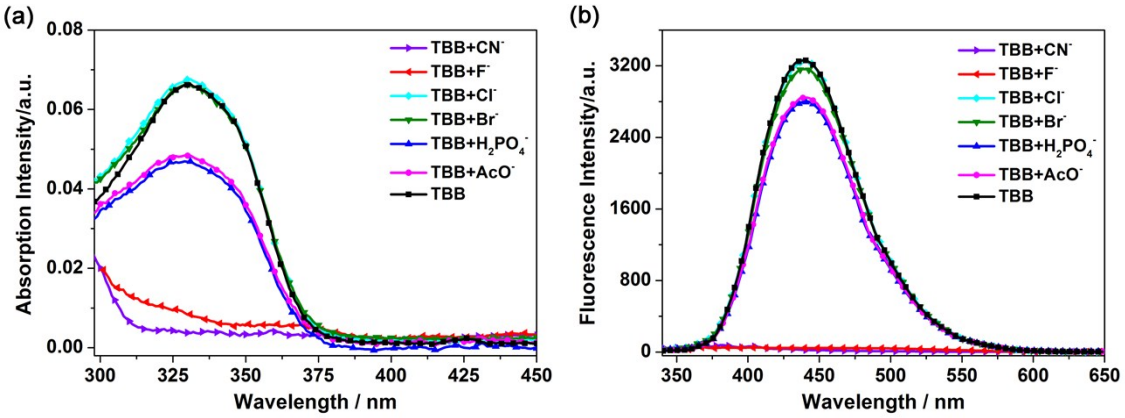

Fig. S30. Absorption (a) and PL (b) spectral changes of **TBB** (2.45 μM in THF, λ_{ex}=330nm) upon addition of an excess of acetate, phosphate, bromide, chloride, fluoride and cyanide ions in THF solutions (167μM).

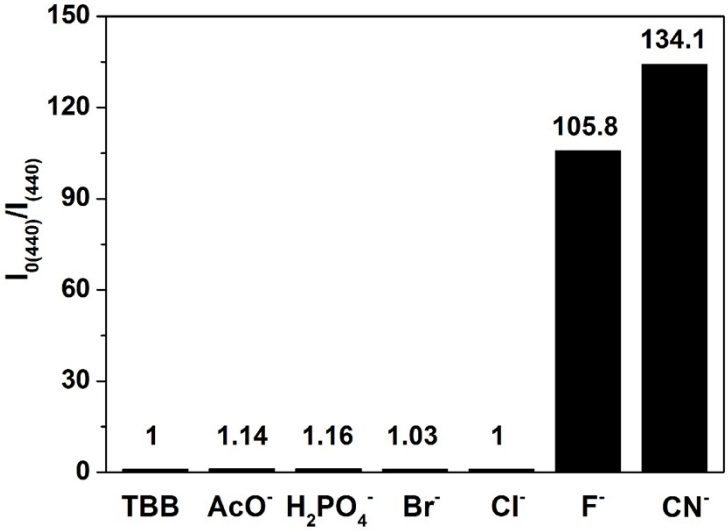

Fig. S31. A comparison of fluorescence intensity at 440 nm of **TBB** in THF solution (2.45 μM) before and after addition of an excess of various anions (167 μM).

High Resolution Mass Spectra.

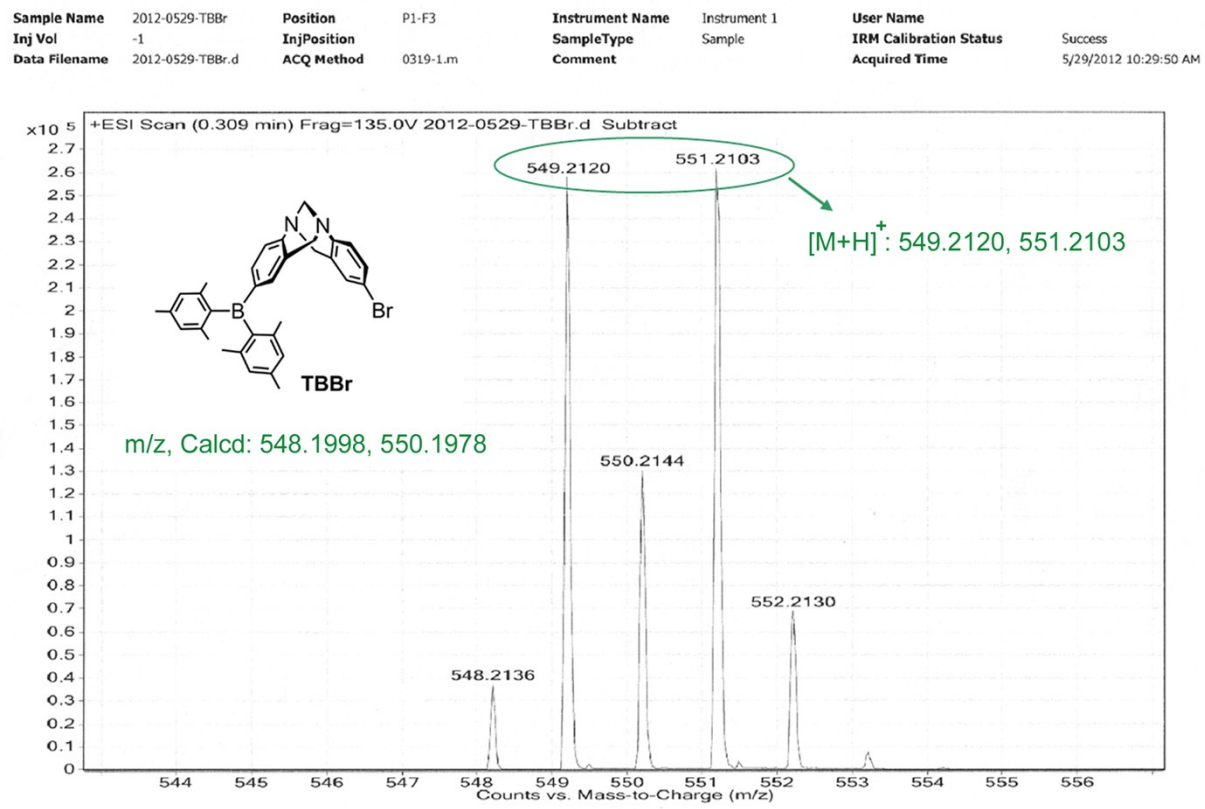

Fig. S32. High resolution mass spectra of **TBBr**.

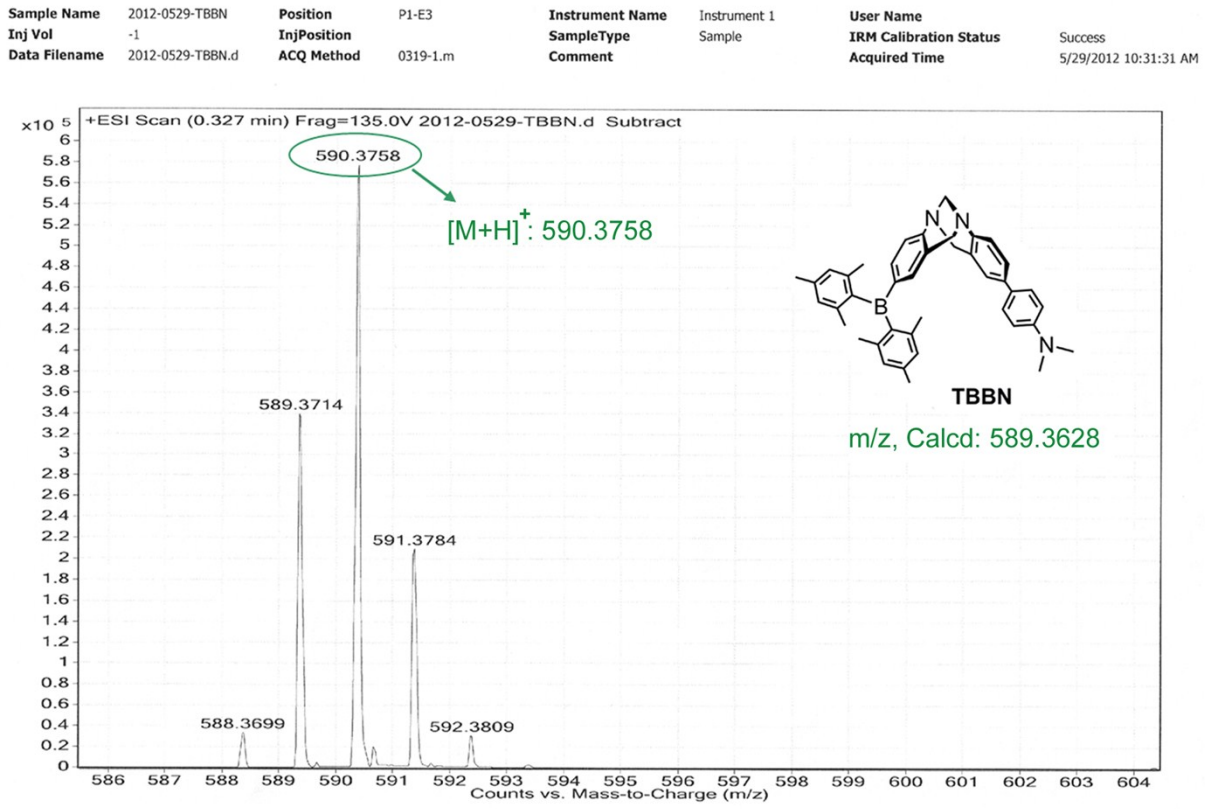

Fig. S33. High resolution mass spectra of **TBBN**.

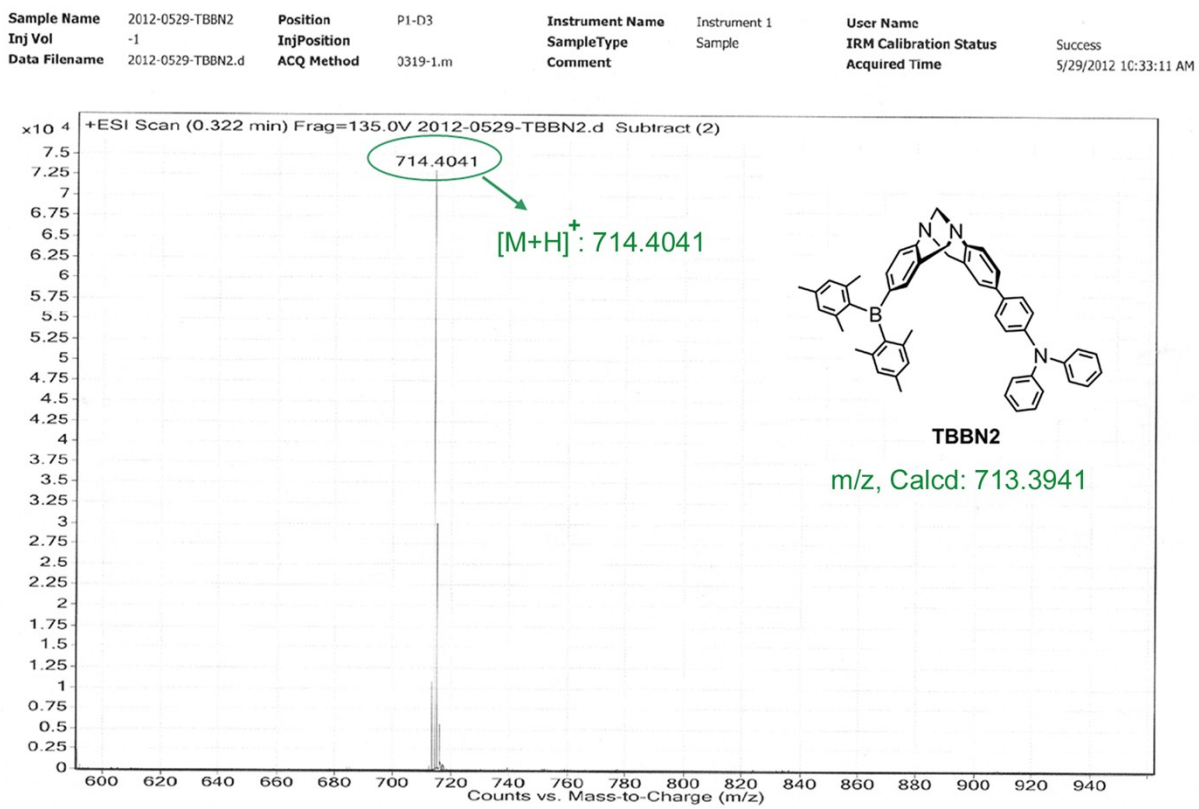

Fig. S34. High resolution mass spectra of **TBBN2**.

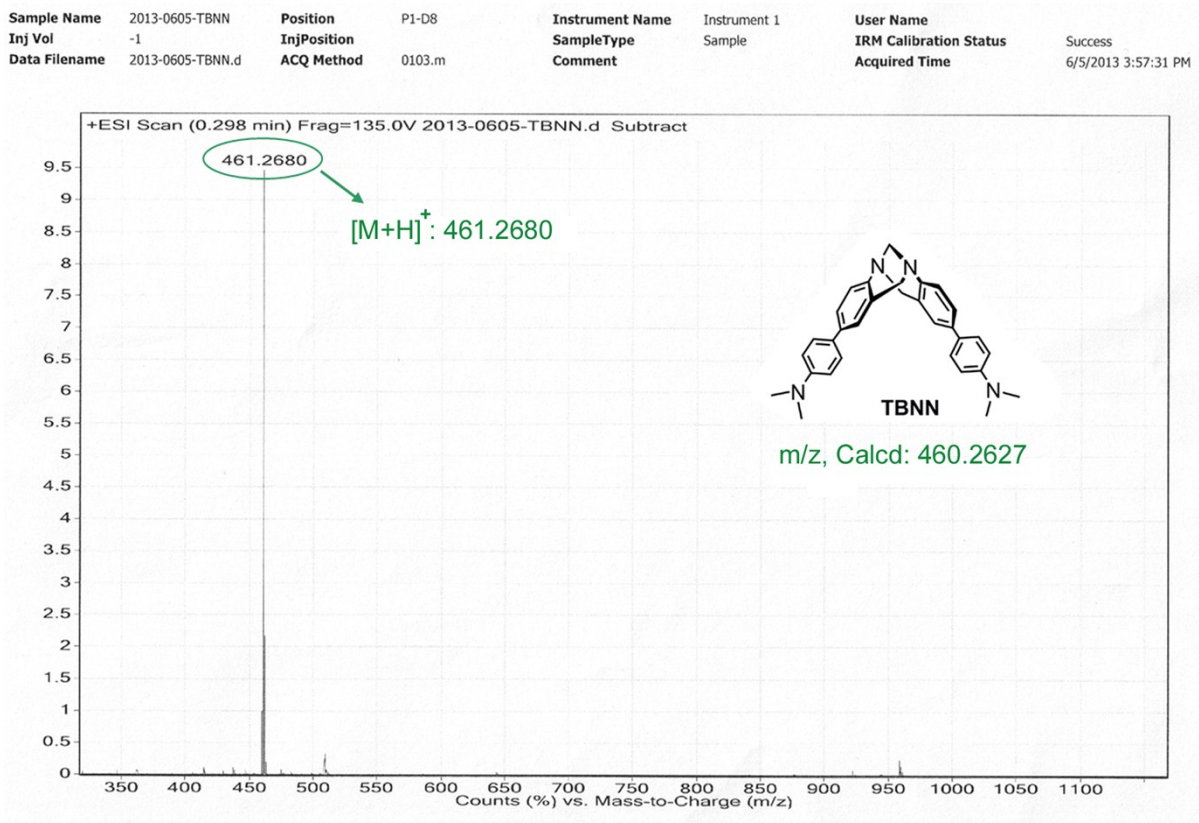

Fig. S35. High resolution mass spectra of **TBNN**.

Reference

(1) Connors, K. A. *Binding Constants*; John Wiley and Sons: New York, 1987.